Pertanika J. Sci. & Technol. 25 (S): 89 - 100 (2017)

PERTANIKA JOURNALS

SCIENCE & TECHNOLOGY

Journal homepage: http://www.pertanika.upm.edu.my/

Microstructure and Mechanical Properties of Hybrid Super ElasticNiTi Alloy with Steel Rebar for Reinforced Concrete Beam

Nubailah Abd. Hamid[1]*, Muhammad Akmal Ahmad Shazalli[2], Muhammad Hussain Ismail[2] and Azmi Ibrahim[2]

[1]Faculty of Civil Engineering, Universiti Teknologi MARA (UiTM), 40450 Shah Alam, Selangor, Malaysia
[2]Faculty of Mechanical Engineering, Universiti Teknologi MARA (UiTM), 40450 Shah Alam, Selangor, Malaysia

ABSTRACT

NiTi is well known for its shape memory effect and super elasticity (SE), and is widely used in medical, dentistry and aerospace applications. For shape memory, NiTi has the ability to undergo deformation at certain temperature then recover to its original shape while SE occurs at narrow temperature range just above its transformation temperature. It shows that this material remembers its original shape and is elastic under stress. The application of nitinol as partial replacement in reinforced concrete beam for seismic resistant structures is popular due to it re-centring capability and distinctive properties. Using Shape Memory Alloy (SMA) in structures has its downsides. Hence, hybrid reinforced concrete beam with SMA was introduced to improve the structure's ductility and energy dissipation. Hence, this research is aimed at distinguishing microstructure and mechanical properties of SMA and steel rebar. Not much is known about how SMA behaves when subjected to compression. Therefore, X-Ray Diffraction (XRD) was used to analyse if any secondary phase exists and Differential Scanning Calorimetry (DSC) test was used to analyse the phase transformation. The results showed hybrid NiTi-steel rebar can address some deficiencies of NiTi and in terms of costs. On the other hand, combining them will result in super elastic recovery, displacement ductility and strength capacity for seismic resistant design.

Keywords: Hybrid NiTi, shape memory alloy, shape memory effect (SME), superelasticity (SE)

ARTICLE INFO

Article history:
Received: 05 January 2017
Accepted: 17 January 2017

E-mail addresses:
*nubailah_hamid@yahoo.com (Nubailah Abd. Hamid),
park_jan11@yahoo.com (Muhammad Akmal Ahmad Shazalli),
muhammadhussain_ismail@yahoo.co.uk (Muhammad Hussain Ismail),
azmii716@yahoo.com (Azmi Ibrahim)
*Corresponding Author

ISSN: 0128-7680

INTRODUCTION

Shape memory alloys (SMAs) are metals that remember their original shapes. They are useful as actuators, which are materials that "change shape, stiffness, position, natural

frequency, and other mechanical characteristics in response to temperature or electromagnetic fields" (Rogers, 1995). The potential use of SMAs, especially as smart rebar, as partial replacement in reinforced concrete beam can provide insights into the development of this material for seismic resistant design and broadened the spectrum of this research into many scientific fields. The diverse applications for these metals have made them increasingly important and visible to the world. This study focused on NiTi since the alloys have been found to be the most useful of all SMAs. The objectives of this study are to determine the mechanical properties of as well as compare super elastic nickel titanium and steel rebar under compressive loading. The properties of NiTi in terms of its hardness and microstructure will be discussed.

There have been many studies on the equilibrium phase diagram of the Ni–Ti system. The phase diagram of Ni-Ti alloy system is important for heat treatments of the alloys and improvement of its shape memory characteristics (Zanaboni, 2008). The author focused on the central region of the phase diagram situated around the equiatomic NiTi composition. The reason is that solid solution B2 austenite phase of a near-equiatomic Ni-Ti alloy exhibits a unique behaviour based on the reversible martensitic. In Figure 1, the right boundary of B2 phase is almost vertical. On the other hand, there is pronounced solubility of Ni atoms in NiTi intermetallic on the Ni-rich side in the temperature range between 830°C and 1310°C. At temperatures below 650°C, there is a very narrow NiTi-phase region, and it is generally accepted that this region accommodates composition only between 50.0 and 50.5% Ni (Rogers, 1995). The NiTi phase retains the B2 order until a low temperature when the martensitic transformation occurs.

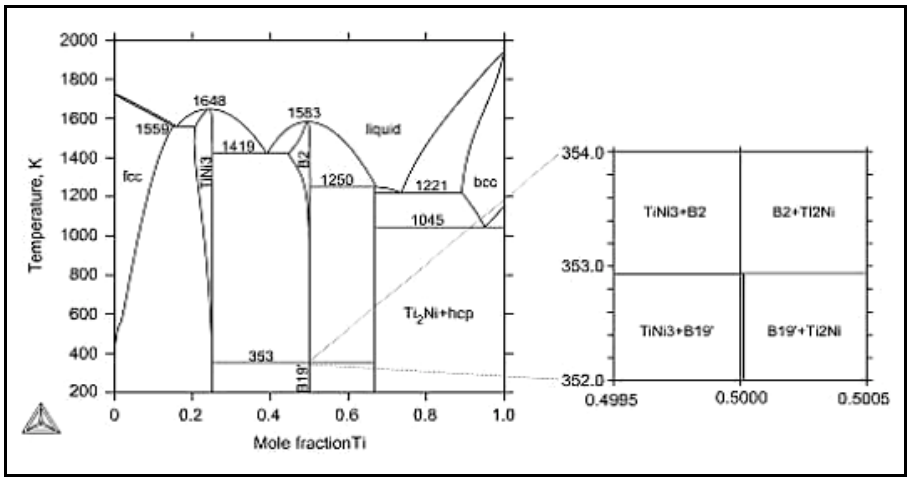

Figure 1. Calculated phase diagram of NiTi binary system, in which the phase equilibrium between B2 and B19S phases is added together with stable phase $NiTi_2$ and NiTi (Kubenova, 2014)

MATERIALS AND METHOD

Materials

NiTi samples used for the experiment was manufactured in China and the material carefully selected and heat treated to ensure it exhibits super elastic response at room temperature. NiTi used was A_f -6.3, with circular cross section of 8mm in diameter and the nominal composition were 56.02% Ni and 43.89% Ti with grain size 8. In addition, 10 mm diameter bars of mild steel rebar with f_{yk} (characteristic strength of 500 MPa) was also prepared for comparison. The standard specimens of Ni-Ti alloy and mild structural steel were fabricated according to ASTM E8/E8M-09 (2009a), and their length was 10 mm.

Cutting of the Specimen

The machinability of NiTi significantly depends on the cutting speed and feed rate, which are typically very high. According to Elahinia, Andani and Haberland (2014), the machining process of the NiTi alloys is quite difficult and challenging despite their properties and resistance to deformation that can cause severe tool wear. In addition, machining NiTi components with high cutting feed and speed will help to extend their tool life and improve product quality, although these elevated speeds result in hardening of the subsurface zones of the part (Weinert & Petzoldt, 2004). Hence, by taking into account these factors, non-conventional machining was employed, where abrasive methods such as grinding and saws were selected. Thus, an abrasive cutter machine was used to cut the NiTi and mild steel rebar into 10 mm for each sample.

Surface Cleaning Process

In order to get a flat smooth surface, samples of NiTi from China and mild steel rebar were subjected to a grinding process. The grinding process of each sample required five grades of abrasive sandpaper in order to obtain the smooth surface and to remove the scar resulting from the cutting process. The grade of the sand paper starts from coarse to fine which are 240, 320, 400, 600 and 1200. The smooth and near mirror image will be helpful in order to get a clear image of the microstructure of samples. After finishing the process of grinding the specimen, the latter was polished using a polishing machine. The cleaning alumina powder was used. The alumina powder consists of four grades starting from 10 µm, 5 µm, 3 µm. For the final finish, the 1µm alumina powder was used. This cleaning agent helped in order to get the mirror look for the sample. Then, the samples were dried using an air compressor to prevent any rust from occurring on the surfaces.

Mechanical Behaviour Test - Monotonic Compression Test and Hardness Test

The behaviour of the SE of material was analysed through monotonic compression test in order to compare the mechanical properties of SMA and steel. All the tests were performed at room temperature using a 250 kN Servo Hydraulic Fatigue Testing System Instron 8802 equipped

with a data acquisition system as shown in Figure 2. Some equipment incorporated in this test were universal testing machines driven by mechanical screw to apply the load with hydraulic systems testing machine, and the Vernier Caliper was used to measure the compressive sample.

Compression tests on SMA are important. Furthermore, little is known about super elastic SMA when subjected to compression. Therefore, a minimum of two samples for each different condition was prepared to observe the behaviour of the samples upon the exertion of maximum stress. This compression test was conducted according to the standard of ASTM E9, and the above-mentioned loading protocol was input using Blue Hill 2 software. The dimension of the samples before and after the compression was measured, and the compression speed was 0.2505 mm/m.

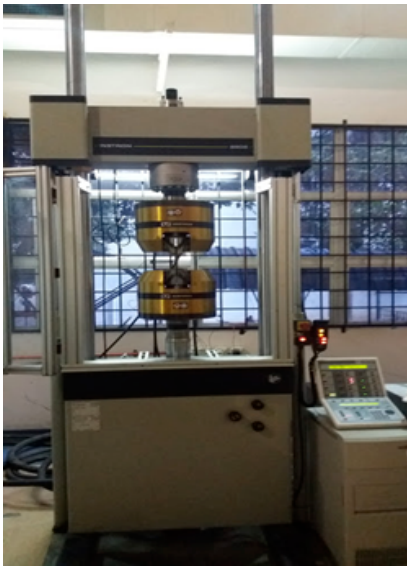

(a)

(b)

(c)

Figure 2. (a) Servo hydraulic fatigue testing system Instron 8802 and standard compression sample for (b) steel rebar (c) NiTi

In order to measure the micro hardness of the samples, Vickers micro hardness test were conducted with 4.9 N of load applied within 15 seconds according to Mortagy and Farag (2007). In addition, nano-indentation was recommended to be used instead of micro-indention in spite of the fact micro hardness readings were influenced by elastic recovery and yield true hardness values (Cheng, 2004).

Phase Analysis - Scanning Electron Microscopy (SEM), Differential Scanning Calorimetry (DSC) and X-Ray Diffraction (XRD)

The phase analysis of both specimens was obtained through the XRD, SEM and DSC analysis. In order to observe the effect of the microstructure on the sample, SEM analysis was used. In this test, backscattered image whereas the SEM that uses mainly secondary electrons to image the specimen, rather than secondary electrons was used. The purpose of conducting this test was to identify the type of microstructure. The samples again were polished using silicon powder and ground using 240, 320, 600 and 1200 abrasive grit paper as mentioned in the XRD section. Polishing can produce a mirror-like image for the microstructure of the samples which was carefully analysed using the 80× and 500× magnifications.

The samples were analysed using DSC to analyse its transformation temperature. The machine used in this research was the DSC-1 Mettler Toledo, a different scanning calorimetry machine. The samples were crushed to obtain mass between 7 mg to 10 mg to be placed in the DSC capsules (Bansiddhi & Dunand, 2009). The samples heated and later cooled at a rate of 10oC/min under nitrogen cover gas. Two DSC cycles ranging from -50 to 200°C were performed consecutively for each sample and the second cycle was used to determine the transformation enthalpy and the phase transformation temperatures.

The purpose of conducting the XRD is to identify its phase and its composition present in all the samples using the RigakuUltima IV. Before the XRD process began, the specimen was ground using the 240, 320, 600 and 1200 abrasive grit papers and was polished using the polishing powder to obtain reflective surface. A wavelength of 1.540562A with a diffraction angle from 30 to 90 at scanning speed of 0.5/min was used to perform the analysis. The peak observed in the XRD result was compared with the phase of NiTi alloy to identify the phase composition of the samples.

RESULTS AND DISCUSSION

Mechanical Behaviour Test - Compression Test and Hardness Test

Figure 3 shows the failure of NiTi samples with differences sizes of diameters. For this test, samples diameter of 8 mm and 12 mm were used. The maximum load for the 8 mm diameter sample was 138.346 kN and the maximum compressive stress obtained is 2752.307 MPa at 31.58%. The result obtained for NiTi 12 mm samples is 239.954 kN with lower compressive stress reading obtained as compared to 8 mm diameter samples at 29.29%, was 2121.656 MPa as expected as stated by Desroches (2004), that the small diameter of shape memory alloys show higher strength and damping properties as compared with the higher diameter of bars.

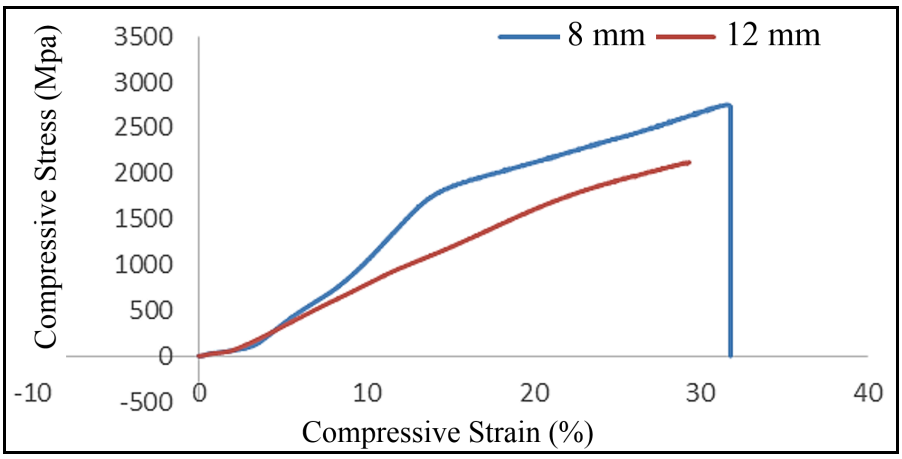

Figure 3. Compressive Stress-Strain curve for 8 mm and 12 mm of NiTi

Table 1
Hardness value for NiTi alloy and mild steel rebar

Point	NiTi alloy (HV)			Mild Steel rebar (HV)		
	D1	D2	Hardness	D1	D2	Hardness
1	76.2	78.9	308.3	84.1	85.4	253.2
2	79	80.4	292.2	92.9	100.3	198.8
3	76.7	78	310.1	82.8	85.1	258.3
4	83.1	79.7	280.1	90.7	92.3	225.4
5	74.6	7.9	327.7	89.5	90.7	2228.4

Table 1 shows the value of hardness for a sample of NiTi and Mild Steel rebar at different points determined by using Vickers hardness test. By referring to the study made by Kaya (2014), he stated that the hardness of a material refers to the strength of the material and the change in the strength is related to the formation of precipitates. For a mild steel rebar sample, at the different point of the test, it gave a different value of hardness. Thus, an average value of hardness for mild steel repair was 232.82. Meanwhile, for NiTi, the value of hardness was also similar with mild steel where each point gives a different reading. Therefore, an average value of hardness calculated was 303.68 HV. Based on data collected, there were similarities of two samples which recorded the highest value of hardness located at the centre of the sample. Bain (1997-1908) reported a slight difference of hardness value obtained from same sample each time during an experiment. There are few factors that affect the differences between each point such as grains, defects, grain boundaries and impurities of the specimen itself. The microhardness was measured by the residual area after load was removed. In the case of the super elastic materials, the elastic part was recovered upon load removal causing a decrease in the size of the residual area resulting in the hardness value appearing larger.

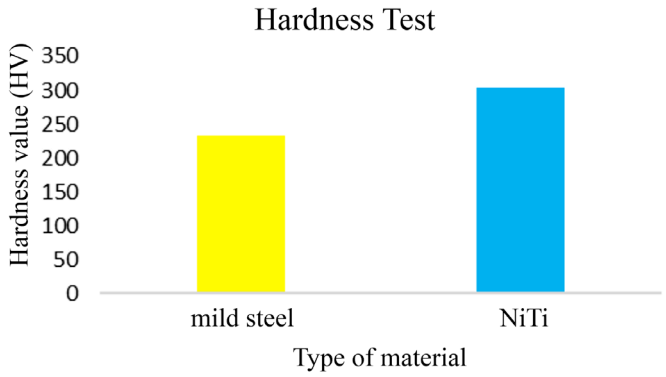

Figure 4. Average of hardness value

Figure 4 shows the data of average hardness value of mild steel rebar and NiTi alloy. It shows a slightly difference in hardness value for mild steel rebar and NiTi where the latter shows higher hardness value compared with mild steel. The differences between both samples were about 13.2%. From the test, it showed that the NiTi alloy has greater resistance to deformation compared with mild steel rebar due to greater hardness. From the SE aspects, the higher the hardness, the higher the SE. This is because SE depends on the strength of the matrix which is affected by the existence of dislocations, precipitates or both. The hardness of the material is also affected by the microstructure and composition of element in material. This is discussed in detail in the XRD and SEM analysis.

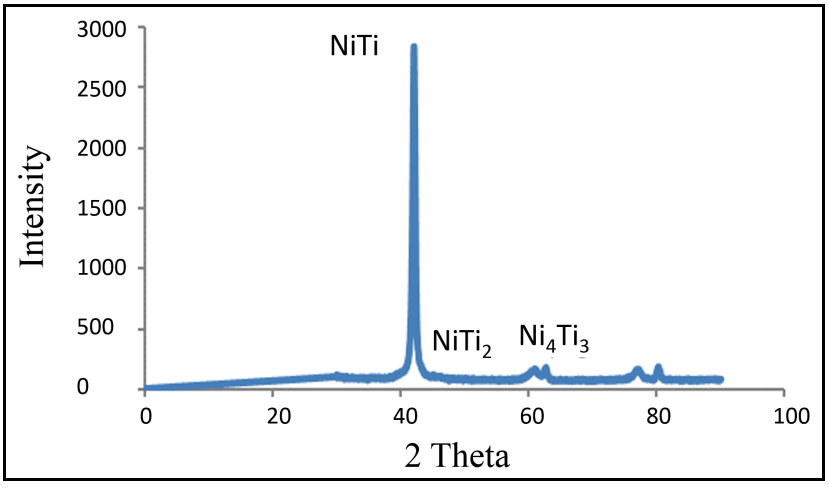

Figure 5. XRD analysis of NiTi

Figure 5 shows the result of received samples of NiTi which is nickel rich, revealing the existence of phase, namely NiTi at the maximum wave peak. The value of the intensity of the maximum peak was 2 thetas, 42.1°. The graph also shows the presence of the secondary phase of $NiTi_2$ and Ni_4Ti_3. Each phase has a different condition where for NiTi it is in a stable phase. Mortagy and Farag (2007) stated that presence of Ni_4Ti_3 is important in order for an improvement in SE behaviour. It gives effect in terms of size, density, and coherency of Ni_4Ti_3 itself. For the $NiTi_2$ phase, Mortagy and Farag (2007) concluded that the presence of $NiTi_2$ does not give effect in terms of mechanical behaviour and SE. Therefore, their existence was negligible in this study.

Meanwhile, Figure 6 shows the phase exists in the mild steel rebar where at maximum wave peak, constructive interference are Fe_3C. By referring to the phase diagram of the Iron-Iron Carbide, the Fe_3C shows that the phase is iron carbide or its other name cementite. The carbon content was about 6.67% C. This intermetallic compound is metastable; it remains as a compound indefinitely at room temperature. It is the hardest structure that appears on the diagram and the crystal structure was orthorhombic. The phase has a low tensile strength, but high in compressive strength.

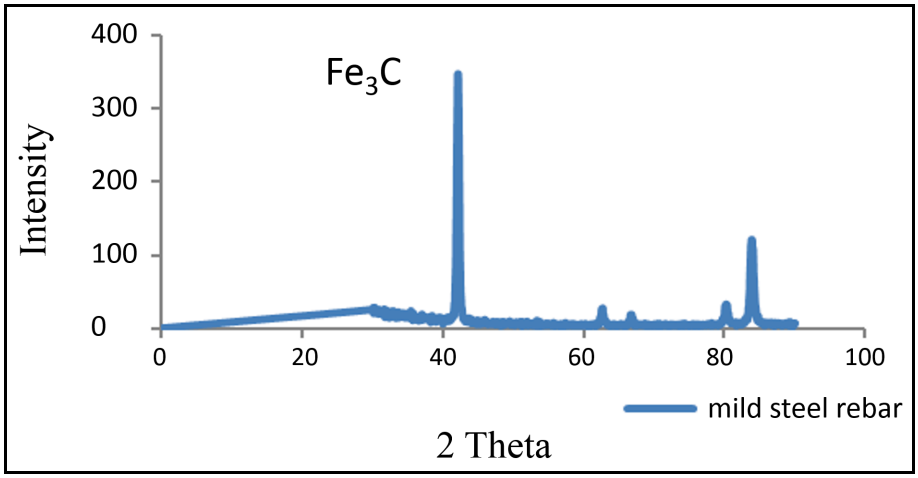

Figure 6. XRD analysis of mild steel rebar

Scanning Electron Microscopy (SEM)

Azimi et al. (2011) pointed to two categories of fracture, ductile and brittle. Ductile fractures are defined as slow tearing of the material with the expenditure of considerable energy, displaying a dimpled surface created by growth of internal voids of the metal and an appreciable gross plastic deformation. Brittle fracture on the other hand is characterised by a rapid rate of crack propagation (due to fluctuating stress cycles), with no gross deformation.

From the study, the main difference in the microstructure of the samples is the topography of surface where it classified both material as either brittle or ductile. Figure 7 and 8 show the fracture image of both material which reveal their characteristics. For the NiTi, the topography

image at the surface of the samples shows that the material undergoes brittle behaviour. This image may explain the graph produced in compression test where the graph declines sharply after the material fails.

Energy-dispersive X-ray spectroscopy (EDX) was conducted to obtain the chemical characterisation of each sample. By doing EDX, it reveals the presence of element in material and its composition. For NiTi samples, the composition of nickel elements at that particular area was about 56.99% while for titanium, it was 43.01%. Some points that were observed through EDX for NiTI sample also showed the same result, whereby the composition of nickel was higher than titanium. This proved the received sample of NiTi is Ni rich.

Figure 8 shows the fracture image of mild steel rebar that also underwent EDX. The topography surface shows that the material underwent ductile behaviour. Azimi et al. (2011) revealed that ductile fracture decreases the diameter of the sample, called necking. It begins after the ultimate stress reaches its maximum level. So, a neck is formed as the sample of mild steel is elongated. The EDX result shows two main element exists in mild steel rebar, carbon and iron. The carbon percentage was about 22.21% while the iron about 70.80%. So, the composition of iron is higher compared with carbon.

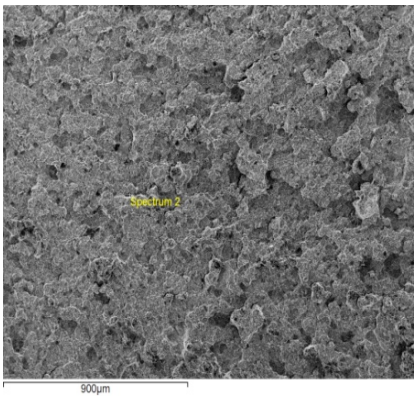

Figure 9. Fracture of NiTi

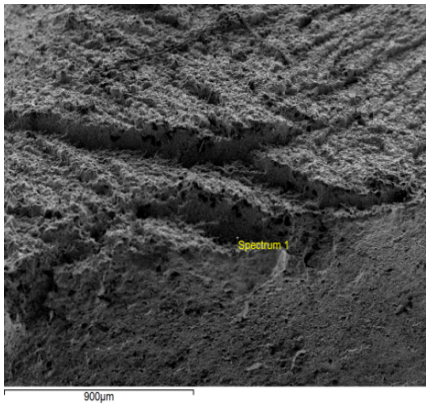

Figure 8. Fracture of mild steel rebar

The formation of a neck introduces a triaxial state of stress in the region. A hydrostatic component of tension acts along the axis of the specimen at the centre of the neck region. Many fine inclusions form in this region which grow and coalesce into a central crack. This crack grows in a direction perpendicular to the axis of the instrument until it approaches the surface of the instrument. The central crack which forms early tends to concentrate the deformation at its tip in narrow bands of high shear strain.

Differential Scanning Calorimetry

For the Ni-rich NiTi, the austenite transformation during heating starts at a temperature of -24.42°C. The austenite finishes at -19.47°C as shown in Figure 9. The size of the peak will determine the SE characteristic of NiTi. Therefore, the wider the peak, the greater the SE behaviour of NiTi. Meanwhile, for the cooling curve, it represents the transformation of martensitic. The onset of the peak represents the martensite start temperature (Ms). The end set of the peak represents the martensite finish temperature (Mf). The transformation of martensitic during cooling starts at -3.06°C and ends at a temperature of -49.46°C.

Figure 10 shows the DSC curve for measuring phase transformation temperature for mild steel rebar. Same with the DSC curve of NiTi, mild steel rebar also contains two curves which represent heating and cooling conditions of the samples. For heating, there is a small peak.

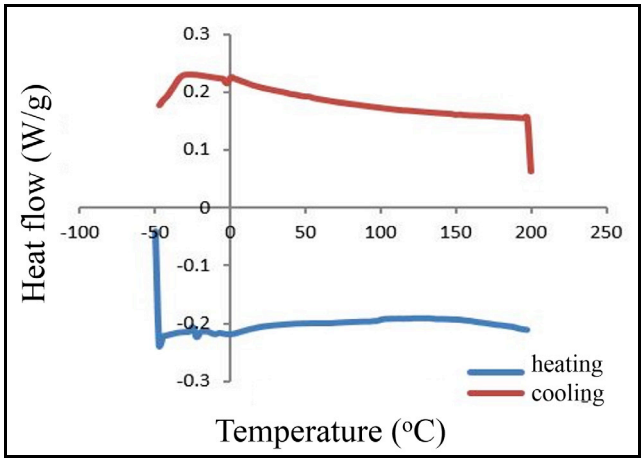

Figure 9. DSC curve for NiTi

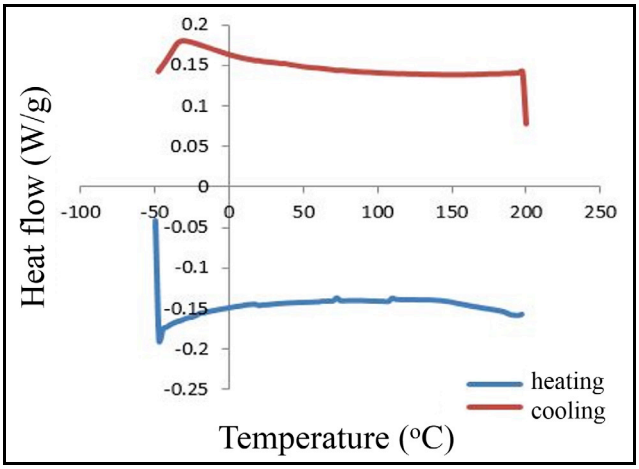

Figure 10. DSC curve for mild steel rebar

CONCLUSION

In this study, the mechanical properties of both materials were identified. The comparison between phase constituent of super elastic nickel titanium and mild steel rebar was conducted. The correlation between both materials in order to see the potential of the materials to be hybrid was found. A few conclusions can be drawn. First, can be clearly seen from the graph of stress vs. strain, the elastic modulus of NiTi is lower compared with mild steel rebar. So, NiTi has a lower stiffness. Second, the hardness for NiTi is higher compared with mild steel rebar. The microstructure of the samples has influences result of hardness test. It can be proven through DSC and SEM test the effect of the structure on the materials, Last but not least, the phase transformation for NiTi was relatively wide, particularly during cooling, which contributed to Ni-rich composition. The Ni content influences the transformation temperature.

The results obtained from this research hopefully will help the researchers in identifying the mechanical characteristic of the materials.

ACKNOWLEDGMENTS

The authors acknowledge the research grants provided by Ministry of Education, 600-RMI/FRGS 5/3 (22/2013), and UiTM internal grant 600-RMI/DANA 5/3/PSI (141/2013), 600-RMI/DANA 5/3/CIFI (29/2013) to undertake this research.

REFERENCES

Azimi, S., Delvari, P., Hajarian, H. C., Saghiri, M. A., Karamifar, K., & Lotfi, M. (2011). Cyclic fatigue resistance and fractographic analysis of RaCe and ProTaper rotary NiTi instruments. *Iranian Endodontic Journal, 6*(2), 80-85.

Bain, R. (1996-1997). *Detailed Report on Hardness Test,* Rine Engineering Pvt Limited: Baddi, India.

Bansiddhi, A., & Dunand, D. C. (2009). Shape-memory NiTi–Nb foams. *Journal of Materials Research, 24*(06), 2107-2117.

Cheng, F. T. (2004). On the indeterminacy in hardness of shape memory alloys. *Journal of Materials Science and Technology*, 700-702.

Elahinia, M., Andani, M. T., & Haberland, C. (2014). Shape memory and super elastic alloys. *High Temperature Materials and Mechanisms, 355*.

Kaya, I. (2014). Shape memory behaviour of single and polycrystalline nickel rich nickel titanium alloys.

Kuběnová, M. (2014). Příprava a martenzitickétransformaceslitinnabáziNiTi.

Mortagy, O., & Farag, M. (2007). Effect of heat treatment on the superelasticity and hardness of NiTi. *In International Conference on Modeling and Optimization of Structures, Processes and Systems (ICMOSPTS'07)*, Durban.

Rogers, C. (1995). Intelligent materials. *Scientific American, 273*(3), 122-5.

Weinert, K., & Petzoldt, V. (2004). Machining of NiTi based shape memory alloys. *Materials Science and Engineering: A, 378*(1), 180-184.

Zanaboni, E. (2008). One way and two way-shape memory effect: Thermo-mechanical characterization of Ni-Ti wires. *UniversitadegliStudi di Pavia, Pavia*, Italy.